How Well Can Simulation Predict Protein Folding Kinetics and Thermodynamics?

Christopher D. Snow,[1] Eric J. Sorin,[2] Young Min Rhee,[2] and Vijay S. Pande[1,2]

[1]Biophysics Program, [2]Department of Chemistry, Stanford University, Stanford, California 94305; email: pande@stanford.edu, csnow@alum.mit.edu, ymrhee@stanford.edu, esorin@stanford.edu

Key Words folding rate, molecular dynamics, transition state ensemble, P_{fold}, reaction coordinate

■ **Abstract** Simulation of protein folding has come a long way in five years. Notably, new quantitative comparisons with experiments for small, rapidly folding proteins have become possible. As the only way to validate simulation methodology, this achievement marks a significant advance. Here, we detail these recent achievements and ask whether simulations have indeed rendered quantitative predictions in several areas, including protein folding kinetics, thermodynamics, and physics-based methods for structure prediction. We conclude by looking to the future of such comparisons between simulations and experiments.

CONTENTS

INTRODUCTION: GOALS AND CHALLENGES

Although several questions relate to the "protein folding problem," including structure prediction (1, 94) and protein design, this review concentrates on another aspect of folding: How do proteins fold into their final folded structure? Experimentally characterizing the detailed nature of the protein folding mechanism is considerably more difficult than characterizing a static structure. We turn to the combination of experiment and atomistic models (that can readily yield the desired spatial and temporal detail), and ask how quantitatively predictive are these simulations? The true test is statistical significance. The very act of statistically comparing simulations with experiments is critical and leads to either model validation or refinement.

Simulating protein folding remains challenging. The most straightforward approach, molecular dynamics (MD) simulations using standard atomistic models (e.g., force fields such as CHARMM, AMBER, or OPLS), quickly runs into a significant sampling challenge for all but the most elementary of systems. Whereas small proteins fold on the multiple microseconds to second timescale, detailed atomistic simulations are currently limited to the nanosecond to microsecond regime. To overcome this barrier, researchers must choose between simplified models and alternate sampling methods, both of which introduce new approximations. We emphasize that the relevant question is not whether a given method is "correct" in some absolute sense (as all models have limitations), but whether the model is predictive.

In the following sections, we review several approaches and ask to what extent these simulations have yielded statistically predictive results. For organizational purposes we consider first the prediction of kinetics, then the folding pathway, and finally the prediction of thermodynamics, including native state structure.

PREDICTIONS OF FOLDING RATE

Impetus and Methods of Rate Assessment

The most accessible quantitative observables of two-state proteins are folding rate, unfolding rate, and thermodynamic stability. Thus, it is important to validate any simulation method through quantitative comparisons with experiments with proper statistics. As rates and free energies are the natural quantitative experimental measurements, relative or absolute prediction of these quantities is necessary for a direct connection to experiment and a true assessment of theoretical methodology.

Rate Predictions from Topology-Based Models

Plaxco and coworkers (85, 86) studied the relationships between polymer length, native state stability, and native topology using folding rates for two dozen small, two-state, single-domain proteins. To quantify native state topology, they defined

the relative contact order (CO) of a protein fold as

$$CO = \frac{1}{L \cdot N} \sum_N \Delta L_{i,j}, \qquad 1.$$

where L is the sequence length, N is the total number of inter-residue, nonhydrogen, atomic contacts within 6.0 Å, and $\Delta L_{i,j}$ is the sequence separation of contacting residues i and j. Significant correlations (R = ~0.9) were observed between native topology (CO) and experimentally determined folding rates, which strongly suggest a link between global native structure and folding kinetics. Whereas the effective folding rate of small two-state folders was previously predicted to be $\ln[k_{eff}] = a + b \cdot CO$, this fit offers little insight into the folding mechanism or the general properties that make CO predictive.

More recently, many theories for the possible origins of the predictive capabilities of CO and the cooperativity inherent to two-state folders have been suggested; because of space limitations, we describe only three of these theories. The zipper model of Muñoz et al. (79) was one of the first works to predict the folding rates for a large range of proteins. Models in this class relate the free energy to the number of native segments present, where folding propagates outward along the sequence from an initial nucleus. This model and more sophisticated generalizations are successful in predicting folding rates and illustrate the link between topology and rate (43). Debe and coworkers (22) used a generic protein Monte Carlo simulation method to sample compact and semicompact protein conformations for sequences of length L, comparing each observed conformation with ~20 heterogeneous native folds (also of length L) and looking for matches in global backbone topology (21, 23). Their results suggest that the native topomer can be found in a diffusive search of the conformational space without a specific mechanism to enhance the sampling. Finally, Plaxco and coworkers (73) derived a relationship between the number of native contacts N and the effective folding rate that simplifies to the CO correlation. Kinetic Monte Carlo simulations using this model (as a Gaussian chain) result in first-order kinetics in which the rate-limiting step is the formation of the N contacts in the native topology (74), thus giving a physical interpretation of the observed two-state kinetics for small proteins.

Rate Predictions from Simulated Dynamics

Analytic models of protein folding differ from standard simulation methods, such as MD and Langevin dynamics, owing to a lack of specificity arising from intramolecular interactions, which must be included through approximate means. This specificity is likely needed for the understanding of sequence-specific effects. With that in mind, we now turn to rate predictions that are made using atomistic potentials on the basis of various approximations of the physics of interatomic interactions (including especially solvent-mediated interactions). As the use of continuum representations of the solvent greatly decreases sampling time, the use of such models has become widespread. The most common electrostatic

treatments are the generalized Born (GB) equation (87) and the distance-dependent dielectric (29). For our purposes, we consider rate predictions under these models collectively. The following discussion begins with implicit solvent rate predictions and is followed by a discussion of the limited number of rate predictions made using explicit representations of the solvent.

SIMULATIONS IN CONTINUUM SOLVENT WITH LOW VISCOSITY   Caflisch and co-workers (28) have pioneered long atomistic folding simulations using simple, computationally efficient implicit solvent models. By using low (or no) viscosity in their simulations, they accelerate the timescales involved in folding and are able to observe multiple folding transitions. Such reversible folding transitions are excellent evidence that sampling is sufficient for useful thermodynamic analysis. However, like any approximation, low-viscosity simulations have limitations, which we discuss below.

In the initial study by Caflisch and coworkers (28), the α-helical $(AAQAA)_3$ peptide and the β-hairpin-forming sequence V_5DPGV_5 were simulated using the united atom CHARMM force field (8) and a distance-dependent dielectric/solvent-accessible surface area (SA) solvent model with $\varepsilon(r) = 2r$. From their combined sampling of $\sim$4 μs for these peptides at multiple temperatures (270 to 510 K), Arrhenius behavior was seen at low temperatures, with mean folding times (inverse folding rates) for the helix and hairpin predicted to be 3.41 and 95.6 ns at 300 K (extrapolated from simulations at or above 330 K, the coldest temperature at which folding was tractable in the study). As noted by the authors, their implicit solvent model did not account for solvent viscosity, and the lack of solute-solvent friction in their simulations makes these folding times lower bounds on the true folding times.

Using the methodology described above, Caflisch and coworkers studied two additional secondary structural motifs: the α-helical $Y(MEARA)_6$ peptide (44) and Beta3s, a three-stranded antiparallel β-sheet (30). Surprisingly, the helical peptide, which contains more helical content (and thus helical stability) than the $(AAQAA)_3$ peptide, folded much more slowly at 300 K, with a mean folding time of $\sim$80 ns. For Beta3s, a mean folding time of 31.8 ns was predicted at 360 K, and a following study predicted a folding time of 39 ns at 330 K (10), both of which are significantly faster than the $\sim$5 μs timescale at lower temperatures reported by De Alba et al. (19). Increased sampling of Beta3s in four additional simulations, each with a length of 2.7 μs or greater, extended the predicted folding time using this model to $\sim$85 ns at 330 K. Additional simulations were also conducted to study the folding of the Beta3s mutant with the two sets of turn GS residues replaced with PG pairs (31), with the mutant folding three times as fast as Beta3s. These inverse folding times thus remain rather high.

This raises the question of whether researchers can use low-viscosity simulation and scaling arguments to predict folding rates. A nonlinear relationship between folding time and viscosity was reported by Zagrovic et al. (116) for the folding kinetics of a 20-residue tryptophan (Trp)-cage miniprotein in the GB/SA implicit
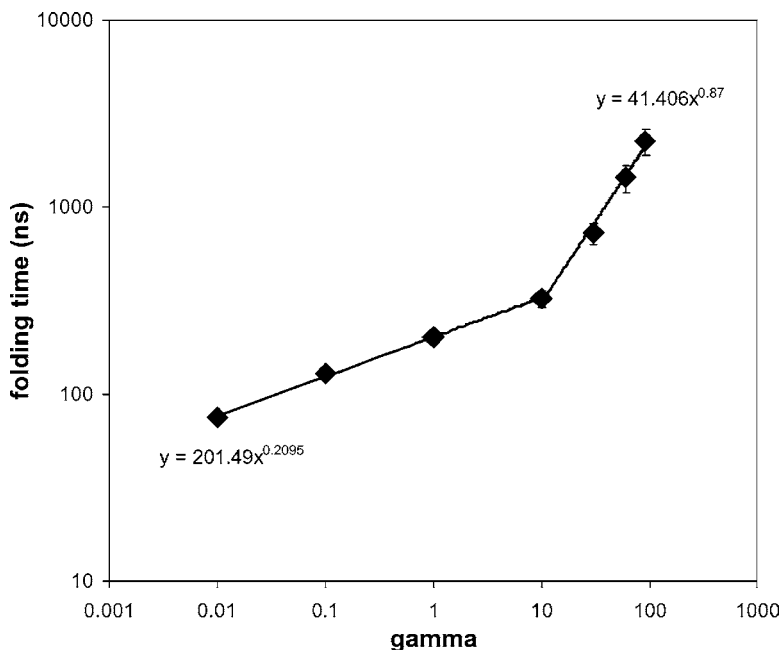
Figure 1 Viscosity dependence of the folding time of the Trp-cage molecule in implicit solvent. The folding times and associated errors were calculated using the maximum likelihood approach. Folding times and viscosities are given relative to the folding time in water and the viscosity of water, respectively. The error bars given are errors propagated on the basis of the Cramer–Rao errors for the individual folding times.

solvent model of Still et al. (87) under a range of solvent viscosities. Figure 1 plots the observed relationship between inverse rate ($\tau = 1/k$) and viscosity ($1/\gamma$) relative to the case for water-like viscosity with $\gamma_{water} = 91$ ps^{-1} (115). Linear scaling of the folding time with solvent viscosity holds for viscosities as low as $\sim 1/10$ that of water; however, below this point the time scales as $t \sim \gamma^{1/5}$. Although applying such scaling rules to the rate predictions of Caflisch and coworkers in low viscosity would bring their values closer to experimentally established rates for these systems, the precise effect of low viscosity for each of these systems remains unclear.

What is the significance of this nonlinearity? The idea that low-viscosity simulations do not adequately capture the folding kinetics may be a sign of further inadequacies in such a model. The lack of solvent viscosity may lead to fast collapse to a nonnative globule with folding proceeding from this globule. Simulations with water-like viscosity collapse on longer timescales and may anneal interatomic contacts prior to collapse. Plaxco & Baker (84) studied folding of the

IgG binding domain of protein L experimentally and via simulation as a diffusive barrier-crossing event. Their findings indicate that the rate-limiting step was strongly correlated with solvent viscosity, with negligible internal friction. Thus, neglect of solvent viscosity in protein folding simulations, while allowing for determination of an upper bound on relative folding rates, may significantly affect the observed folding mechanism.

SIMULATIONS IN CONTINUUM SOLVENT WITH WATER-LIKE VISCOSITY   Including viscosity significantly increases the required sampling time, yet with water-like viscosity, absolute folding kinetics can be measured directly. To this end, Pande and coworkers (82) have applied distributed computing to sample trajectory space stochastically and to extract rates from an ensemble dynamics perspective. Two-state behavior is the central concept upon which rates are extracted via ensemble dynamics; dwell times in free energy minima of the conformational space are significantly longer than transition times (i.e., barrier crossing is much faster than the waiting period). The probability of crossing a barrier that separates state A from state B by time t is thus given by

$$P(t) = 1 - e^{-kt}, \qquad\qquad 2.$$

where k is the folding rate. In the limit of $t \ll 1/k$, this simplifies to $P(t) \approx kt$ and the folding rate (according to the Poisson distribution) is given by

$$k = \frac{N_{folded}}{t \cdot N_{total}} \pm \frac{\sqrt{N_{folded}}}{t \cdot N_{total}}. \qquad\qquad 3.$$

For example, if 10,000 simulations are each run for 20 ns and 15 of them cross a given barrier, we obtain a predicted rate of $k = 0.075(\pm 0.019) \ \mu s^{-1}$, which corresponds to a folding time of $13.3(\pm 3.4) \ \mu s$. In this way, Pande and coworkers can use many short trajectories to investigate the folding behavior of polymers that fold on the microsecond timescale: As shown previously, using M processors to simulate folding results in an M-times speedup of barrier-crossing events (100). When $t > 1/k$, as is the case for helix formation and other fast processes, ensemble convergence to absolute equilibrium can be established, and the complete kinetics and thermodynamics can be extracted simultaneously.

In several recent studies, Pande and coworkers have utilized implicit solvent models while maintaining water-like viscosity via a Langevin or stochastic dynamics integrator with an inverse relaxation time γ. In the first study (118), they introduced a method of "coupled ensemble dynamics" as a means to simulate the ensemble folding of the C-terminal β-hairpin of protein G (1GB1) using the GB/SA continuum solvent model of Still et al. (87) and the OPLS united atom force field (56) with water-like viscosity. A total sampling time of $\sim$38 μs was obtained, with a calculated inverse folding rate of $4.7(\pm 1.7) \ \mu s$, in agreement with the experimentally determined value of 6 μs (79).

Other hairpin structures have been studied by the Pande group more recently, both in an effort to gain insight into hairpin folding dynamics and for a more

thorough comparison with experimental measurements. They reported folding and unfolding rates for three Trp zipper β-hairpins (104) using the methodology described above, including TZ1 (PDBID 1LE0), TZ2 (PDBID 1LE1), and TZ3 (PDBID 1LE0 with G6 replaced by D-proline). As shown in Table 1, the relative inverse folding rates are in good agreement with experimental fluorescence and infrared measurements provided by experimental collaborators. Unfolding rates were also predicted with relatively strong agreement.

Beyond these investigations of simple hairpin subunits, several small proteins were studied with an implicit solvent methodology. The first, a 20-residue

TABLE 1 Comparing corrected simulation protein inverse folding rates with experiment[a]

System	Force field	Solvent	T (K)	τ_{fold} (μs)	τ_{exp} (μs)
C-terminal 1GB1 β-hairpin	OPLSua	GB/SA	300	4.7($\pm$1.7)	6
TZ1 (PDBID 1LE0)	OPLSaa	GB/SA	296	5–7	6.25
TZ2 (PDBID 1LE1)	OPLSaa	GB/SA	296	3–6	2.47
TZ3 (1LE0, replacing G6 with P)	OPLSaa	GB/SA	296	2–6	0.83
Trp cage (PDBID 1L2Y)	OPLSua	GB/SA	300	1.5–8.7[b]	4
BBA5 single mutant	OPLSua	GB/SA	298	16	<10
BBA5 double mutant	OPLSua	GB/SA	298	6	7.5($\pm$3.5)
Villin headpiece	OPLSua	GB/SA	300	5	4.3($\pm$0.6)
C(AGQ)W (W quenching)	AMBER-94	TIP3P	300	0.076($\pm$0.006)	0.073
	CHARMM22	TIP3P	300	0.127($\pm$0.006)	0.073
C-terminal 1GB1 β-hairpin	CHARMM22	TIP3P	300	5	6
Engrailed homeodomain[c]	ENCAD	F3C	373	O(0.010)	0.005–0.025
Fs peptide	AMBER-99ϕ	TIP3P	305	0.016–0.020	0.016($\pm$0.005)
BBA5	AMBER-GS	TIP3P	298	7.5($\pm$4.2)	7.5($\pm$3.5)
Villin headpiece	AMBER-GS	TIP3P	300	10.0($\pm$1.7)	4.3($\pm$0.6)

[a]Predictions described in the text for which no reasonable experimental comparison can be made have been left out of the table.

[b]Based on a range of alpha carbon RMSD cutoffs from 2.5 to 3.0 Å.

[c]Thermal unfolding rates, rather than folding rates, are compared.

miniprotein known as the Trp cage, has an experimental folding time of ∼4 μs. From simulations totaling ∼100 μs the folding rate was estimated on the basis of a cutoff parameter in alpha carbon RMSD (root mean-squared displacement) space: $k_{fold}(3.0\ \text{Å}) = (1.5\ \mu\text{s})^{-1}$; $k_{fold}(2.8\ \text{Å}) = (3.1\ \mu\text{s})^{-1}$; $k_{fold}(2.7\ \text{Å}) = (5.5\ \mu\text{s})^{-1}$; $k_{fold}(2.6\ \text{Å}) = (6.9\ \mu\text{s})^{-1}$; and $k_{fold}(2.5\ \text{Å}) = (8.7\ \mu\text{s})^{-1}$. Although the predicted folding time roughly agreed with the experimental value, the calculations illustrated the dependence of rates upon definition of the native state (to minimize this dependence cutoffs must be chosen along an optimal reaction coordinate). Post analysis of ensemble folding data is not necessarily trivial unless there are many folding events and a stable native ensemble is easily distinguished from decoys with similar topology. Similar rate predictions were made for two mutants of the 23-residue BBA5 miniprotein and compared with temperature-jump measurements made by the Gruebele laboratory (103). A single mutation replaced F8 with W, which acts as the fluorescent probe, and the double mutant also included a replacement of V3 with Y. As shown in Table 1, the agreement between simulation predictions and experimental measurements was excellent for the double mutant at 6 μs and 7.5($\pm$3.5) μs, respectively. The agreement was less striking in the case of the single mutant, for which experiment offered an upper limit of 10 μs and simulation predicted 16 μs, with a range of 7 to 43 μs on the basis of the alpha carbon RMSD cutoff used.

One of the most notable simulation studies to date is the tour de force 1 μs trajectory of the villin headpiece conducted by Duan & Kollman (26). Pande and coworkers have simulated the ensemble folding of this 36-residue three-helix bundle (PDBID 1VII) using the GB/SA continuum solvent and the OPLS united atom force field in water-like viscosity (117). With over 300 μs of simulation time, the folding time was predicted to be 5 μs (1.5 to 14 μs using alpha carbon RMSD cutoffs from 2.7 to 3 Å, as described above), which was compared with the 11 μs folding time derived from nuclear magnetic resonance (NMR) lineshape analysis. A follow-up study by Eaton and coworkers (61a) tested the prediction using temperature-jump fluorescence and found the folding time to be 4.3($\pm$0.6) μs, validating the rate prediction.

Is this method a panacea for addressing long timescale dynamics? The direct observation of folding kinetics presents difficulties, especially for larger proteins or those without single-exponential behavior. For example, folding ensembles generated from a single unfolded model attempt to populate the unfolded ensemble and observe folding. However, the timescale involved for the initial equilibration and the timescale necessary for chain diffusion across the folding barrier scale dramatically with chain length (61). These factors make it increasingly difficult to observe both equilibration and folding for large proteins. In addition, Paci et al. (80) have shown that folding events in extremely short trajectories can proceed from high-energy initial conformations. Deviations from two-state behavior can also make interpretation of ensemble kinetics difficult (33), and given the short timescale of current folding simulations (10 to 1000 ns), any obligate intermediate with an appreciable dwell time (1 to 100 ns) may represent a sufficient deviation.

Fortunately, these challenges may not be intractable: The timescale for downhill equilibration to a relaxed unfolded ensemble may require long simulations, but should be much faster than folding. Also, the detection of intermediates and multiple pathways can be accomplished by the comparison of folding and unfolding ensembles. Finally, these concerns may also be addressed with new Markovian state model methods (102, 110).

Regardless of the relatively strong agreement between ensemble simulations in implicit solvent and experimental rate measurements, several factors must be considered in interpreting such simulation results. Lacking a discrete representation of water, these studies ignore the potential role that aqueous solvent might play in the folding process. Furthermore, the compact nature of the relaxed unfolded state ensembles observed using the GB/SA solvent model may pose problems for the folding of larger proteins, such as artificial trapping in compact unfolded conformations.

RATE PREDICTIONS IN EXPLICIT SOLVENT   Although simulating folding in explicit solvent remains a daunting task, a number of results have recently been published [most often employing rigid three-point water models such as TIP3P (54) or SPC (3)]. The use of such models can add insight into the dynamics of biologically relevant solutes; however, it must be stressed that the added computational demand imposed by explicit solvent models does not necessarily equate with added accuracy in the resulting simulations (for example, in comparison with the results that employ implicit water models described above), and several shortcomings inherent to these models are known. Most importantly, commonly used water models have generally been parameterized to a single temperature ($\sim$298 K) and poorly capture the temperature dependence of important properties such as the solvent density and diffusion coefficient (45). Improved representations of the solvent usually add to the required processing time. Thus, the use of explicit water models generally involves simple solvent models at or near ambient/biological temperature.

Even simple explicit water models greatly limit the simulation timescale for a solute of given molecular size, and it is not surprising that rate predictions using such models have previously been limited to the most rapid events. Hummer et al. (48, 49) studied helix nucleation in the A_5 and A_2GA_2 peptides using the TIP3P model at temperatures from 250 to 400 K, placing the nucleation event on the 100 ps timescale, in good agreement with the upper bound of 100 ps reported by Thompson et al. (111). Yeh & Hummer (114) also studied loop closure kinetics in the $C(AGQ)_nW$ peptide (n = 1, 2) using the AMBER-94 (14) and CHARMM22 (72) force fields to compare simulated intrachain contact rates (based on tryptophan triplet quenching by cysteine) with the experiments of Lapidus et al. (63). Although the resulting conformational distributions between the two force fields differed significantly, the predicted quenching times faired well compared with the experimental result of 73 ns: AMBER-94 predicted 76 $\pm$ 6 ns and CHARMM22 predicted 127 $\pm$ 6 ns after correction for the viscosity difference between the simulations and experiments.

While these studies offer insight into the most elementary events in protein folding, a number of studies have recently been published on the formation and/or denaturation of larger protein structure. Daggett and coworkers (75, 76) have reported unfolding rate predictions using explicit solvent models with direct experimental comparisons. The 61-residue engrailed homeodomain (En-HD) forms a three-helix bundle similar to that of the villin headpiece and undergoes thermal denaturation at 373 K with a half-life of 4.5 to 25 ns. Mayor et al. (75, 76) simulated the thermally induced unfolding of En-HD using the F3C water model (66) in ENCAD (65) at this temperature with an unfolding rate on the tens of nanoseconds timescale. The time needed to reach the putative transition state at 75 and 100°C, 60 ns and 2 ns, respectively, was roughly consistent with the extrapolated experimental unfolding rates. Precise rates cannot be extracted from a single unfolding event because of the stochastic nature of protein dynamics.

Bolhuis (5) thoroughly simulated the folding of the C-terminal β-hairpin of protein G using a stochastic transition path sampling methodology. Bolhuis employed the transition interface sampling method to extract transition kinetics. At 300 K, with an equilibrium constant of $\sim$1, the predicted folding time of 5 μs using the TIP3P explicit solvent is in good agreement with the experimental rate of 6 μs (79) and with the rate predicted by Zagrovic et al. (118) using an implicit solvent. The observed agreement suggests that path sampling will be useful in future simulation studies to elucidate the kinetics and mechanisms inherent to protein folding, and it will be interesting to see such methods applied to larger and more complex systems.

Peptides and miniproteins allow for complete and accurate sampling of folding and unfolding events via simulation at biologically relevant temperatures. Sorin & Pande (105) recently studied the helix-coil transition in two 21-residue α-helical sequences and demonstrated complete equilibrium ensemble sampling for multiple variants of the AMBER force field, thus allowing quantitative assessment of the potentials studied. Observing that the previously published AMBER variants resulted in poor equilibrium helix-coil character compared with experimental measurements, they tested a new variant denoted AMBER-99ϕ and showed that it more adequately captured the helix-coil thermodynamics and kinetics, yielding a predicted helix formation rate of 0.05–0.06 ns^{-1}, in excellent agreement with Williams et al. (112), who derived a value of 0.06 ns^{-1} from temperature-jump measurements.

To study the formation of a more complex protein structure, Pande and coworkers (89) recently reported unbiased folding simulations of the 23-residue miniprotein BBA5 in explicit solvent. Ten thousand independent MD simulations of the denatured conformation of BBA5 solvated in TIP3P water resulted in an aggregate simulation time of over 100 μs. This sampling yielded 13 complete folding events that, when corrected for the anomalous diffusion constant of the TIP3P model, result in an estimated folding time of 7.5($\pm$4.2) μs. This is in excellent agreement with the experimental folding time of 7.5($\pm$3.5) μs reported by Gruebele and coworkers (103).

Folding of the villin headpiece was first attempted by Duan & Kollman in 1998 (26). When they used the TIP3P explicit solvent, their single 1 μs simulation did not show complete folding, which is not surprising given the $\sim$5 μs folding time for that protein. Pande and coworkers (G. Jayachandran, V. Vishal & V.S. Pande, manuscript in preparation) have recently observed folding of this protein using the TIP3P water model and the AMBER-GS force field at 300 K, thus increasing the maximum sequence size of proteins for which simulated folding has been observed with MD. With a total sampling time of $\sim$0.5 ms, a folding time of $10(\pm1.7)$ μs was predicted using a particle mesh Ewald treatment of long-range electrostatics. Identical simulations using a reaction field treatment yielded $9.9(\pm1.5)$ μs. These values are somewhat slower than the $4.3(\pm0.6)$ experimental folding time, which might be due to the slow equilibration previously observed for helix formation under the AMBER-GS potential (105).

Closing Statements on Simulated Rate Predictions

Prediction of relative rates (e.g., demonstrating a correlation between experimental and predicted rates) is valuable; however, prediction of the absolute rate without free parameters is a more stringent test. Although calculation of absolute rates is computationally demanding, we expect such absolute comparisons to become more common (for increasingly complex proteins) with the advent of new methods and increasing computer power. Finally, we stress that a quantitative prediction of rates is not sufficient to guarantee the validity of a model. The ability of different models to quantitatively predict folding rates strongly suggests that more experimental data are needed to further validate simulation.

Our focus on in vitro protein folding alone is not intended to detract from the advances seen in related areas. These include, but are not limited to, the characterization of protein folding rates in pores (58), in chaperonins (2), and under force (71), as well as rate predictions for small RNAs (106) and nonbiological polymers (27). Additionally, several coarse-grained calculations have been employed to study folding and unfolding rates (11, 50, 78). Indeed, a number of methodologies are now employed so that researchers may understand the kinetics of protein folding and unfolding, from molecule-specific atomistic simulations to statistical calculations of CO that attempt to characterize rates across a range of systems. A similar spectrum of methods has also been applied to folding mechanism, as discussed below.

IDENTIFYING THE PATHWAY FOR PROTEIN FOLDING

Identifying Transition State Structures or Intermediates

Determining which structures belong to the transition state ensemble (TSE) is a difficult task and a vigorous subfield. Our discussion focuses on the two-state case, in which a single transition state connects the folded and unfolded ensembles. The

techniques we discuss are relevant to each transition present in more complex scenarios. We first discuss means of selecting transition state conformations: unfolding simulations, projection onto one or two reaction coordinates, validation of putative transition states through calculation of P_{fold}, and path sampling. We then discuss validation of transition state conformations: the interpretation of experimental Φ values (Φ_{exp}) and the prediction of Φ_{sim} values. Because of space constraints we do not discuss the inverse approach, the use of Φ_{exp} restraints to generate TSEs.

CONFORMATIONAL CLUSTERING OF HIGH-TEMPERATURE TRAJECTORIES   Unfolding simulations are powerful tools (16). The Daggett group has used a clustering method for picking transition state structures that relies on the presence of a large conformational change after the transition. They first compute the pairwise distance matrix between all structures and produce a two- or three-dimensional representation of the distance between each trajectory snapshot using multidimensional scaling (68). Then, putative transition conformations prior to escape from the native region are manually selected. Although Li et al. (68) modestly suggest that this method is not rigorous, it clearly can be effective, providing a putative chymotrypsin inhibitor 2 (CI2) TSE with a $R = 0.94$ correlation to 11 Φ_{exp} values.

We note that the free energy landscape and the TSE can be altered by denaturant, whether thermal, chemical, or force, and there may be significant differences between the high-temperature and physiological free energy landscape (24, 36). At sufficiently high temperatures the rapid unfolding events observed are for practical purposes irreversible. Fortunately, in many cases the nature of protein unfolding transitions appears largely temperature independent. The Daggett laboratory has examined the temperature dependence for the engrailed homeodomain (En-HD) and CI2 (18, 76). Mayor et al. (75) report that the En-HD transition states determined at 100 and 225°C were similar (the 100°C transition state has $R = 0.86$ correlation to Φ_{exp}). Another study reports that these two putative transition state structures have a $RMSD_{c\alpha}$ of 3.8 Å, more similar to each other than to their respective starting structures (76). To study the temperature dependence for CI2 unfolding, Day et al. performed seven simulations (20 to 94 ns) at varying temperature. The unfolding trajectories had a similar order of events. Whereas the average number of tertiary contacts had large fluctuations, the transition states were essentially the same (171 contacts at 498 K to 174 contacts at 373 K) (18).

What is the temperature dependence of unfolding pathways? Caflisch and coworkers (10) report a weak temperature dependence of the free energy surface for Beta3s. Pande and coworkers have observed similar unfolding landscapes for high temperature unfolding ensembles of tryptophan zippers (C. Snow & V. Pande, unpublished results). Thus, a crucial question is, Why, given the relatively large free energy shift in the transition state induced by high temperature, are the structural properties obtained at high temperature so useful? A possible answer lies in the relationship between native topology and folding mechanism. Given the Hammond postulate, the transition state should increasingly resemble the native

state at higher temperatures. The native topology is important for kinetics (see above) and may typically be reflected in the transition state topology. Given these trends, perhaps high-temperature transition states will deviate significantly only for transition states that diverge strongly from the native topology.

PROJECTION ONTO REACTION COORDINATES   In favorable cases, projection onto one or several parameters, such as the fraction of native contacts present (Q), can produce a free energy landscape that reveals clear differences between the folded and unfolded states. Given a properly weighted equilibrium ensemble, and an optimal projection, the density of states at the saddlepoint would reveal exactly the free energy barrier height, and conformations at the saddlepoint could be flagged transition state members. Both prerequisites are problematic. In the general case, folding transitions cannot be reduced to two dimensions without overlap of kinetically distinct conformations.

One hallmark of this effect is that simplified dynamics on the reduced landscape do not reproduce the correct dynamics. Swope et al. (110) demonstrated altered kinetics and non-Markovian behavior for a carefully produced state space in which all possible native hydrogen bonding patterns in a small β-hairpin were resolved. In a companion paper, a simple nine-state example reveals how non-Markovian behavior arises on short timescales when nine microstates are lumped into three macrostates (109). It is not trivial to construct order parameters meaningful for kinetics, yet such order parameters are crucial for a Markovian description.

These challenges notwithstanding, accurate projection of simulations onto reaction coordinates has been pursued by many researchers. For example, Onuchic and coworkers studied several proteins by using Gō models. They demonstrated reversible Gō model folding for CI2, Src SH3, barnase, RNase H, and Che Y, qualitatively matching experimental observations (13). They successfully extended these models to large proteins, dihydrofolate reductase, and interleukin-1β (12). Koga & Takada (59) adopted and extended the Onuchic Gō models to a set of 18 small proteins to test the predicted TSE and folding rates by projection onto Q. They found topology-influenced rates that were roughly comparable to experiment, and qualitatively reasonable Φ_{sim} value predictions in about half of the systems. More recently, they studied the folding of protein G and α-spectrin SH3 using a hybrid potential that includes Gō character and sequence-specific physical bias (64) and found qualitative agreement with experimental mechanism.

COMMITTOR PROBABILITIES: P_{fold} Large conformational transitions for proteins are both slow and stochastic. Nevertheless, the direct computation of the transmission coefficient (P_{fold}) for putative transition state conformations has become possible in various cases. P_{fold}, defined as the probability that a conformation reaches the folded state before it reaches the unfolded state (25), is computationally expensive because, to compute this probability precisely, many simulations are performed from identical coordinates with randomized initial velocities. The relative error for the calculated P_{fold} from N trials scales with $N^{-0.5}$. Thus 20 trials

estimate the P_{fold} within 22% of the mean. Another difficulty is that the timescale necessary for commitment to the free energy minima can be long. This spontaneous relaxation rate is related to the timescale for downhill folding scenarios and the prefactor for transition state folding theories.

We expect topology and chain length to play an important role in the relaxation time (61). For Gsponer & Caflisch (41), 16 of 60 P_{fold} simulations for Src SH3 required more than 100 ns to observe commitment, and 6 of 60 had not reached either minimum after 200 ns. These are long commitment times considering their simple no-viscosity implicit solvent but make sense in the context of a sizable β-sheet protein. In contrast, Pande and coworkers (89) observed commitment times under 5 ns for the 23-residue BBA5 in explicit and implicit solvent. Returning to a large explicit water simulation, Daggett and coworkers (20) did not observe commitment to either the native or unfolded state for initial CI2 structures within the putative TSE (within 3 ns).

In comparison, Gō model P_{fold} calculations are tractable. Li & Shakhnovich (70) used an all-atom Gō model to construct and verify a TSE for CI2 using 20 P_{fold} calculations ($N = 20$) per putative transition state (800 total). Shakhnovich and coworkers (7) also elegantly demonstrated reversible folding and unfolding for the C-Src SH3 domain using a coarse-grained Gō model. Putative TSE members were validated by calculation of 100 P_{fold} simulations for each initial model. Finally, the Shakhnovich group has also developed a heavy atom Gō potential and reconstructed the TSE for CI2 (70), protein G (47, 99), and the ribosomal protein S6 (46).

Computing P_{fold} values removes some of the uncertainty when selecting the TSE members, ensuring that one does not select a transition state that is predisposed to either free energy minimum. Although the results are insensitive to details of the cutoffs inside minima, the gross definitions are still important. We must also recognize that bias can influence the selection of putative transition conformations and that conformations subject to Φ_{exp} value restraints may lack the full variation in orthogonal degrees of freedom such as the number of contacts, radius of gyration (R_g), or RMSD (46).

Bolhuis et al. (6) have developed rigorous path sampling techniques that tackle these issues directly. After a large ensemble of transition paths are constructed, statistical analysis determines which conformations have $P_{fold} = 0.5$. An advantage of this method is that researchers can obtain a TSE without presupposing a reaction coordinate. No assumptions about the nature of the transition are necessary; it is only necessary to describe cutoffs for folding and unfolding. Likewise, clustering of MD ensembles into a Markovian model may allow the simultaneous determination of all rates in the system and the identification of the TSE without assignment of the reaction coordinate (102).

Experimental Means to Identify TSE Structures

EXPERIMENTAL PROBES OF THE TSE: Φ VALUES   Φ values allow the interpretation of experimental kinetics for a series of mutants in terms of ground state and

transition state structure for two-state transitions (34). To produce well-defined results, the mutations must perturb significantly the equilibrium free energy of unfolding. The necessary size of this perturbation has been a recent topic of contention (35, 91). The reliability of the Φ value at a given site can be improved by making multiple mutations at a given site. Sosnick and coworkers (60) employ a continuum of energetic perturbations using clever chemistry to measure Ψ values. Despite significant energy perturbation, the mutations should not perturb structural properties. This may seem trivial given the plasticity of the hydrophobic core of proteins (93). However, Burton et al. (9) found that a single-point mutation can induce sizable changes in the transition state. Furthermore, proteins are cooperative; the deletion of several amino acids can rapidly denature a protein. The folded and unfolded thermodynamic minima have dramatically different structural properties, but the free energy balance for unfolding, ΔG_u, is usually small for two-state proteins of less than 100 residues.

VALIDATION OF PUTATIVE TRANSITION STATE STRUCTURES VIA Φ VALUES   Comparisons of Φ_{sim} and Φ_{exp} values have been reported with correlation coefficients as high as R = 0.94 (more than 11 residues) (68). Do high correlation coefficients imply that we can predict Φ_{exp} values? Gō models biased toward the native state structure predict Φ_{exp} values well. Accordingly, we ask to what extent Φ value correlations reflect the information content of the native topology. Researchers desire proof that a physical potential improves the predictive capabilities. To spur critical assessment we must answer two questions: How difficult is it to predict Φ_{exp} values to a given correlation value, and to what extent does Φ value correlation validate other simulation details?

Calculation of Φ_{sim} values can be attempted by either a thermodynamic or kinetic approach. To directly mimic experiment, we could, with sufficient sampling, observe the folding and unfolding rate for each of the mutants of interest. This kinetic method has been used in connection with Gō models (95) but has not yet been applied to unbiased MD simulations. Until recently, estimation of the folding rate for even a single system has been too computationally demanding. Most work has employed the thermodynamic approach, simple arguments relating the free energy of mutation to the deletion of methyl groups from the hydrophobic core (93). Typically, estimates for the ΔG of mutation count the contacts made in the transition and native ensembles with $\Phi_{sim} = \Delta N_{TS}/\Delta N_N$. Various definitions of contacts have been used. For example, Li & Daggett (68) count ΔN as the difference in the number of van der Waals contacts made by the wild-type and the mutant residue, where two residues share a van der Waals contact if two heavy atoms come closer than the sum of their van der Waals radii plus 1 Å. The Daggett lab also employs an alternative approximate parameter, the product of the fraction of native secondary structure ($S_{2°}$) and native tertiary structure ($S_{3°}$), or S-value. The secondary structure content is averaged over the preceding and following residues and is based on (φ, ψ) values, as described by Daggett & Levitt (15). Tertiary structure is the ratio of the number of tertiary

van der Waals contacts in the putative transition state to the number in the native state.

The Daggett and Fersht laboratories led the way in the comparison of simulated and experimental transition state structure. The first such study, characterizing the CI2 transition state observed in high-temperature unfolding simulations (67), produced a set of Φ_{sim} values for 10 hydrophobic core mutants with a 0.12 average deviation from Φ_{exp}. A subsequent work reported that the average of four putative transition state conformations yielded a R = 0.94 correlation (68). The CI2 TSE had an R = 0.87 correlation between the S-values and the Φ_{exp} values. In a study of barnase, thermal denaturation S-values roughly correlated (R = 0.75) to the Φ_{exp} values (17, 69). Fulton et al. (38) presented the calculation of S-values for two putative transition state models of FKBP12. A fair degree of variation between the two models resulted in a R = 0.62 correlation between the average S-values and the Φ_{exp} values. If S-values were selected from either transition state interchangeably and the two most problematic residues were neglected, the correlation improved to R = 0.90 (38). In a practical test, the Daggett transition state models have already been employed to successfully design a faster folding CI2 variant via transition state stabilization (62). Moving beyond simple heuristics for calculating Φ_{sim}, Pan & Daggett (81) computed CI2 thermodynamic Φ_{sim} values by free energy perturbation calculations upon the transition and denatured ensembles. The quantitative comparison to experiment was good (R = 0.8 to 0.9). Clementi et al. (13) have also used a thermodynamic approach to calculate Φ_{sim}, measuring the energy of mutation in the unfolded, folded, and transition state ensembles.

The most rigorous calculation of Φ_{sim} values would be the prediction of both thermodynamic and kinetic Φ_{sim} values. Here, Brooks and coworkers (95) have found excellent qualitative agreement for fragment B of protein A (R = 0.87), although the small free energy barrier and the use of a single reaction coordinate led to discrepancies.

Pathway Prediction and Description

The folding pathway is arguably the most interesting prediction associated with folding simulations. As our ability to observe long timescale transitions improves, it becomes increasingly important to clearly communicate the observed mechanism. Qualitative descriptions of the folding pathway can only be loosely interpreted compared with experiment. First, results found in folding simulations can be sensitive to the analysis. For example, Swope et al. (110) produce several folding mechanisms for the hairpin from protein G by varying their hydrogen bond definition. Second, there are semantic issues; a researcher might frame the discussion of β-hairpin folding in terms of zippering, secondary versus tertiary contacts, or diffusion-collision versus nucleation-condensation.

The collaborative effort between the Fersht experimental laboratory and the Daggett simulation laboratory has shed light on an entire family of unfolding mechanisms. The homeodomains, small three-helix proteins, exhibit a spectrum

of folding processes, from concurrent secondary and tertiary structure formation (nucleation-condensation mechanism) to sequential secondary and tertiary formation (framework mechanism) (40). They present putative transition state conformations from high-temperature unfolding for En-HD, c-Myb, and hTRF1 (two at both 373 and 498 K for En-HD; seven at 498 K for c-Myb; and two at 498 K for hTRF1), and estimate β_T values (0.83, 0.83, and 0.8, respectively) that roughly agree with the experimental β_T values (0.83, 0.79, and 0.90, respectively). Excluding the mutation of two charged residues, correlation coefficients of 0.79 and 0.74 for En-HD and c-Myb were obtained between the S- and Φ values. Gianni et al. (40) report that folding of En-HD resembles the diffusion collision mechanism more than folding of c-Myb or hTRF1 does because the helices are nearly fully formed in the transition state. They do state that movements from diffusion-collision to nucleation-condensation are not detected simply by the helical content of the folding transition states but through analysis of whether the secondary and tertiary structures are formed simultaneously (40). Given this strategy we feel it is particularly important to generate a statistically meaningful number of transitions to judge the relative timing of events between related molecules.

It is not trivial to compare simulated mechanism with experiment. Even in the limit of perfect two-state behavior, we may draw a distinction between the prediction of Φ values and the prediction of folding pathway or mechanism. For instance, high Φ values do not necessarily indicate a critical role in nucleation and low Φ values do not preclude the possibility that the residues are involved in nucleation (47).

In the absence of common, quantitative definitions of mechanism, different research groups are reminiscent of the allegorical blind men who encounter and attempt to describe an elephant (possibly, by drawing two-dimensional projections). Each observer may focus on a different aspect. Raw quantitative comparison of trajectory data is difficult owing to the stochastic nature of the dynamics. The order of "events" is a natural description of a mechanism, but an optimal description of a mechanism should account for heterogeneity as well as the interplay between secondary and tertiary contacts. An excellent and recent example comes from protein A. Fersht and coworkers (92, 113) have qualitatively compared several published simulation predictions of the protein A folding pathway with experiment. None of the published atomistic simulations were completely consistent with experiment, emphasizing the need for improved simulation predictions of the folding pathway and improved quantitative means for comparing pathway predictions.

The simulation community would greatly benefit from continuing efforts toward rigorous prediction of experimental observables related to protein folding. For example, the Tanford coefficient is the relative efficacy of denaturant upon the transition state relative to the native state. Currently, this is roughly estimated via the solvent-accessible surface area or the compactness. Native state hydrogen exchange also appears promising and complementary to Φ value analysis. Certainly, an entire hierarchy of states with varied structure provides additional points of

comparison for simulation. Direct prediction of spectroscopic properties is a promising direction. One example was provided by Shimada & Shakhnovich (99), who reconcile apparently contradictory experimental kinetics measurements for protein G by considering ensemble averages designed to mimic the reaction coordinate for fluorescence experiments. Quantitative prediction helps verify simulations, but also can shed light on the best interpretation of experiment.

Folding Dynamics from the Free Energy Landscape

CHALLENGES   Through the knowledge of an accurate free energy landscape along kinetically relevant degrees of freedom, it becomes possible to identify the stable conformations (unfolded, folded, and any stable intermediates) together with the transition state(s) connecting them. The knowledge of the free energy surface can be directly related to thermodynamic quantities (the free energy barrier height) as well as to kinetic information (the ratio between the folding rate and the unfolding rate, or K_{eq}).

RESULTS   In the original landscape approach, as pioneered by Brooks and coworkers (94), the free energy landscape or potential of mean force (PMF) is generated from the equilibrium population distribution. Because it is excessively time-consuming to reach equilibrium for high-dimensional protein molecules with conventional MD, simulations are performed with umbrella sampling. An additional potential (usually a quadratic or "umbrella" potential) is added to the original Hamiltonian of the system to bias the sampling. When the bias is adjusted, the size of the available conformational space can be reduced to expedite the equilibration within the biased Hamiltonian. A series of biased simulations are recombined afterward to remove the bias in a mathematically strict way by the weighted histogram analysis method (32). The population distribution $P(q)$ then can be converted to the free energy with $F(q) = -\ln P(q)$. With this approach, Brooks and coworkers have obtained the free energy landscape and folding dynamics of the α-helical protein A (4), the $\alpha\beta$-mixed GB1 (97, 98), and the mostly β Src-SH3, (96) with numerous successful comparisons with experiment. We refer the reader to an excellent review (94).

Umbrella sampling studies produce informative free energy landscapes but assume that degrees of freedom orthogonal to the surface equilibrate quickly. The MD time needed for significant chain movement could significantly exceed the length of typical umbrella sampling simulations (which are each typically on the nanosecond timescale). However, in spite of this caveat, umbrella sampling approaches have been successful. One explanation for this success lies in the choice of initial conditions: Umbrella sampling simulations employ initial coordinates provided by high-temperature unfolding trajectories. This is a recurring theme: Without lengthy simulations, the initial conformations are crucially important, and it appears that unfolding produces reasonable initial models.

NEW SAMPLING METHODOLOGY   The success of thermodynamic methods rests on sampling the entire available phase space. In addition to the high dimensionality of protein configuration space, kinetic trapping creates a major bottleneck. Although umbrella sampling can partly overcome this difficulty by simulating multiple trajectories at the same time, kinetic trapping or slow orthogonal degrees of freedom may still dominate within each umbrella potential.

A number of techniques have been developed to overcome kinetic trapping. Mitsutake et al. (77) have provided an excellent review of these generalized ensemble methods. We focus on replica exchange molecular dynamics (REMD), which has been widely used in protein folding simulations. In this approach, a number of simulations (replicas) are performed in parallel at different temperatures. After a certain time, conformations are exchanged with a Metropolis probability. This criterion ensures that the sampling follows the canonical Boltzmann distribution at each temperature. Kinetic trapping at lower temperatures is avoided by exchanging conformations with higher temperature replicas. This method is easier to apply than other generalized ensemble methods because it does not require a priori knowledge of the population distribution.

After Sugita & Okamoto (108) demonstrated its effectiveness with a gas-phase simulation of a pentapeptide Met-enkephalin, Sanbonmatsu & García (90) obtained the free energy surface of the same system using explicit water. With 16 parallel replicas they observed enhanced sampling (at least ∼5 times greater sampling) compared with conventional constant temperature MD. Because the method is simple and because it is trivially parallelized in low-cost cluster environments, it rapidly gained wide application. Berne and coworkers (121) applied this method to obtain a free energy landscape for β-hairpin folding in explicit water using 64 replicas with more than 4000 atoms. With the equilibrium ensemble and the free energy landscape in hand, they reported that the β-hairpin population and the hydrogen bond probability were in agreement with experiments, and they proposed that the β-strand hydrogen bonds and hydrophobic core form together during the folding pathway.

If care is taken to fully reach equilibrium (88), REMD becomes powerful for elucidating the folding landscape. For example, García & Onuchic (39) applied the method to a relatively large system, protein A. With 82 replicas for more than 16,000 atoms with temperatures ranging from 277 to 548 K, and with ∼13 ns MD simulations for each replica, they reported convergence to the equilibrium distribution with quantitative determination of the free energy barrier of the folding.

REMD was further developed to include exchanges in multidimensional Hamiltonian space in combination with umbrella sampling (107). It was also adapted to a heterogeneous parallel cluster by multiplexing the replicas in each temperature (88). Nevertheless, it suffers from one significant problem when it is applied to significantly large systems. As can be inferred from the examples described above (82 replicas for protein A versus 16 for Met-enkephalin), the major drawback of the original REMD is the dependence of the number of replicas on the degrees of freedom f in the system. To obtain a reliable result, each pair of adjacent replicas

must have overlapping energy distributions (108). Because the average energy and the fluctuation in the energy scale as $\bar{E} \sim f k_B T$ and $\delta E \sim \sqrt{f} k_B T$, respectively, the temperature difference of adjacent replicas scales as $\Delta T \sim 1/\sqrt{f}$. Thus, an N times larger system requires $\sqrt{N}$ times more replicas. As a remedy, alternative Hamiltonian REMDs have been proposed in which replicas are generated by varying parameters other than the temperature, such as the degree of hydrophobicity of the polymer chain (37), and by using a scaling parameter for selected energy terms such as the dihedral energy and protein-protein nonbonded interactions (52).

Prediction of the Final Structure

STRUCTURE PREDICTION AS METHODOLOGY VALIDATION   Applied native state structure prediction has been a great challenge in theoretical structural biology, and a number of different approaches have been proposed and applied to this end (42). Here, we focus on structure prediction that adopts an MD approach. The main purpose is not simply to predict the native structure, but to validate the methods, particularly the force field. Standard potential sets have accurately identified the native state for a growing menagerie of peptides and miniproteins. Direct relaxation to the native state remains a challenge for proteins of increasing size. As simulation data for various proteins accumulate, we may realize the long-term goal: refinement of the force field parameters for uniformly accurate prediction of many properties beyond the folding characteristics.

PREDICTION OF THE NATIVE STATE   Although the native structure of the protein is governed not by potential energy but by free energy, regions of low potential energy usually constitute the native state ensemble. Such regions have been detected simply by monitoring the potential energy in MD simulations. Jang et al. (51) reported that such an approach with an implicit solvent model (GB/SA) found good agreements between low-energy conformations and experimental native structures for β-hairpin, β-sheet, and $\beta\beta\alpha$-motif with RMSD values of the predicted structures as low as 1.36 Å. Snow et al. clearly identified native tryptophan zippers using the OPLS all-atom force field (55, 56), and the OPLS united-atom force field predicted a nonnative free energy minimum (104). Similarly, Simmerling et al. (101) demonstrated that this scheme could predict a stable structure for the Trp-cage protein. A NMR structure determination reported an inspiring level of agreement between the predicted and determined structures (101). In this report simulations were performed at relatively high temperatures (325 to 400 K) to expedite the search through the available conformational space. The kinetic trapping described above becomes significantly less problematic at such high temperatures.

As the free energy is directly related to the canonical population distribution at a given temperature, it is attractive to use REMD to look for the structure with the most favorable free energy. Pitera & Swope (83) applied REMD to the Trp-cage protein and reported that the global free energy minimum reproduced

the NMR distance restraints. REMD was also used to compare different solvent models. Zhou and coworkers (119, 120) applied REMD to both explicit and implicit solvent models to obtain free energy surfaces in both models and reported that GB continuum solvent models may predict an incorrect free energy global minimum.

Direct structure prediction for larger structures faces a double obstacle: longer folding timescales and the compilation of errors in force fields for large systems. With larger proteins, force field errors should compound at least as fast as the square root of the number of residues, whereas the stability only increases modestly. In large systems, a direct search for the native structure using MD will be problematic when, regardless of barrier height, diffusional search time exceeds current computational power.

CONCLUSIONS

In the end, an understanding of complex biophysical phenomena will require computer simulation at some level. Most likely, experimental methods will never yield the level of detail that can today be reached with computer simulations. However, the great challenge for simulations is to prove their validity. Thus, it is naturally the combination of powerful simulations with quantitative experimental validation that will elucidate the nature of how proteins fold.

How close are we to achieving this goal? In many ways, there has been great progress. The ability to quantitatively predict rates, free energies, and structure from simulations on the basis of physical force fields reflects significant progress made over the past five years. It also draws attention to a new challenge. Even the prediction of experimental observables, such as rates, within experimental uncertainty does not prove that the simulations will yield correct insights into the mechanism of folding. Indeed, recent work suggests that computational models can both agree with experiment and disagree with each other (89).

We must therefore push the link between simulation and experiment further by connecting the two with new observables, multiple techniques, and increasingly strict quantitative comparison and validation of simulation methods. Without more detailed experiments, we may not be able to sufficiently test current simulation methodology and the trustworthiness of refined simulations may remain unclear. Nonetheless, the ability to predict rates, free energies, and structure of small proteins is a significant advance for simulation, likely heralding even more significant advances over the next five years.

The *Annual Review of Biophysics and Biomolecular Structure* is online at
http://biophys.annualreviews.org

LITERATURE CITED

1. Baker D, Eaton WA. 2004. Folding and binding. *Curr. Opin. Struct. Biol.* 14:67–69

2. Baumketner A, Jewett A, Shea JE. 2003. Effects of confinement in chaperonin assisted protein folding: rate enhancement by decreasing the roughness of the folding energy landscape. *J. Mol. Biol.* 332:701–13

3. Berendsen HJC, Postma JPM, van Gunsteren WF, Hermans J. 1981. Interaction models for water in relation to protein hydration. In *Intermolecular Forces*, ed. B Pullman, pp. 331–42. Dordrecht: Reidel

4. Boczko EM, Brooks CL III. 1995. First-principles calculation of the folding free energy of a three-helix bundle protein. *Science* 269:393–96

5. Bolhuis PG. 2003. Transition-path sampling of β-hairpin folding. *Proc. Natl. Acad. Sci. USA* 100:12129–34

6. Bolhuis PG, Chandler D, Dellago C, Geissler PL. 2002. Transition path sampling: throwing ropes over rough mountain passes, in the dark. *Annu. Rev. Phys. Chem.* 53:291–318

7. Borreguero JM, Dokholyan NV, Buldyrev SV, Shakhnovich EI, Stanley HE. 2002. Thermodynamics and folding kinetics analysis of the SH3 domain form discrete molecular dynamics. *J. Mol. Biol.* 318:863–76

8. Brooks BR, Bruccoleri RE, Olafson BD, States DJ, Swaminathan S, Karplus M. 1983. CHARMM: a program for macromolecular energy, minimisation, and dynamics calculations. *J. Comp. Chem.* 4:187–217

9. Burton RE, Huang GS, Daugherty MA, Calderone TL, Oas TG. 1997. The energy landscape of a fast-folding protein mapped by Ala-Gly substitutions. *Nat. Struct. Mol. Biol.* 4:305–10

10. Cavalli A, Ferrara P, Caflisch A. 2002. Weak temperature dependence of the free energy surface and folding pathways of structured peptides. *Proteins* 47:305–14

11. Chavez LL, Onuchic JN, Clementi C. 2004. Quantifying the roughness on the free energy landscape: entropic bottlenecks and protein folding rates. *J. Am. Chem. Soc.* 126:8426–32

12. Clementi C, Jennings PA, Onuchic JN. 2000. How native-state topology affects the folding of dihydrofolate reductase and interleukin-1 beta. *Proc. Natl. Acad. Sci. USA* 97:5871–76

13. Clementi C, Nymeyer H, Onuchic JN. 2000. Topological and energetic factors: What determines the structural details of the transition state ensemble and "en-route" intermediates for protein folding? An investigation for small globular proteins. *J. Mol. Biol.* 298:937–53

14. Cornell WD, Cieplak P, Bayly CI, Gould IR, Merz KM, et al. 1995. A second generation force field for the simulation of proteins, nucleic acids, and organic molecules. *J. Am. Chem. Soc.* 117:5179–97

15. Daggett V, Levitt M. 1992. Molecular dynamics simulations of helix denaturation. *J. Mol. Biol.* 223:1121–38

16. Daggett V, Levitt M. 1993. Protein unfolding pathways explored through molecular dynamics simulations. *J. Mol. Biol.* 232:600–19

17. Daggett V, Li A, Fersht AR. 1998. Combined molecular dynamics and Phi-value analysis of structure-reactivity relationships in the transition state and unfolding pathway of barnase: structural basis

of Hammond and anti-Hammond effects. *J. Am. Chem. Soc.* 120:12740–54

18. Day R, Bennion BJ, Ham S, Daggett V. 2002. Increasing temperature accelerates protein unfolding without changing the pathway of unfolding. *J. Mol. Biol.* 322: 189–203

19. De Alba E, Santoro J, Rico M, Jimenez MA. 1999. De novo design of a monomeric three-stranded antiparallel beta-sheet. *Protein Sci.* 8:854–65

20. De Jong D, Riley R, Alonso DO, Daggett V. 2002. Probing the energy landscape of protein folding/unfolding transition states. *J. Mol. Biol.* 319:229–42

21. Debe DA, Carlson MJ, Goddard WA. 1999. The topomer-sampling model of protein folding. *Proc. Natl. Acad. Sci. USA* 96:2596–601

22. Debe DA, Carlson MJ, Sadanobu J, Chan SI, Goddard WA. 1999. Protein fold determination from sparse distance restraints: the restrained generic protein direct Monte Carlo method. *J. Phys. Chem. B* 103:3001–8

23. Debe DA, Goddard WA. 1999. First principles prediction of protein folding rates. *J. Mol. Biol.* 294:619–25

24. Dinner AR, Karplus M. 1999. Is protein unfolding the reverse of protein folding? A lattice simulation analysis. *J. Mol. Biol.* 292:403–19

25. Du R, Pande VS, Grosberg AY, Tanaka R, Shakhnovich EI. 1997. On the transition coordinate for protein folding. *J. Chem. Phys.* 108:334–50

26. Duan Y, Kollman PA. 1998. Pathways to a protein folding intermediate observed in a 1-microsecond simulation in aqueous solution. *Science* 282:740–44

27. Elmer SP, Pande VS. 2004. Foldamer simulations: novel computational methods and applications to poly-phenylacetylene oligomers. *J. Chem. Phys.* 121:12760–71

28. Ferrara P, Apostolakis J, Caflisch A. 2000. Thermodynamics and kinetics of folding of two model peptides investigated by molecular dynamics simulations. *J. Phys. Chem. B* 104:5000–10

29. Ferrara P, Apostolakis J, Caflisch A. 2002. Evaluation of a fast implicit solvent model for molecular dynamics simulations. *Proteins* 46:24–33

30. Ferrara P, Caflisch A. 2000. Folding simulations of a three-stranded antiparallel β-sheet peptide. *Proc. Natl. Acad. Sci. USA* 97:10780–85

31. Ferrara P, Caflisch A. 2001. Native topology or specific interactions: What is more important for protein folding? *J. Mol. Biol.* 306:837–50

32. Ferrenberg AM, Swendsen RH. 1989. Optimized Monte Carlo data analysis. *Phys. Rev. Lett.* 63:1195–98

33. Fersht AR. 2002. On the simulation of protein folding by short time scale molecular dynamics and distributed computing. *Proc. Natl. Acad. Sci. USA* 99:14122–25

34. Fersht AR, Leatherbarrow RJ, Wells TNC. 1987. Structure-activity relationships in engineered proteins: analysis of use of binding energy by linear free energy relationships. *Biochemistry* 26:6030–38

35. Fersht AR, Sato S. 2004. Phi-value analysis and the nature of protein-folding transition states. *Proc. Natl. Acad. Sci. USA* 101:7976–81

36. Finkelstein AV. 1997. Can protein unfolding simulate protein folding? *Protein Eng.* 10:843–45

37. Fukunishi H, Watanabe O, Takada S. 2002. On the Hamiltonian replica exchange method for efficient sampling of biomolecular systems: application to protein structure prediction. *J. Chem. Phys.* 116:9058–67

38. Fulton KF, Main ERG, Daggett V, Jackson SE. 1999. Mapping the interactions present in the transition state for unfolding/folding of FKBP12. *J. Mol. Biol.* 291:445–61

39. García AE, Onuchic JN. 2003. Folding a protein in a computer: an atomic description of the folding/unfolding of protein A.

Proc. Natl. Acad. Sci. USA 100:13898–903

40. Gianni S, Guydosh NR, Khan F, Caldas TD, Mayor U, et al. 2003. Unifying features in protein-folding mechanisms. *Proc. Natl. Acad. Sci. USA* 100:13286–91

41. Gsponer J, Caflisch A. 2002. Molecular dynamics simulations of protein folding from the transition state. *Proc. Natl. Acad. Sci. USA* 99:6719–24

42. Hardin C, Pogorelov TV, Luthey-Schulten Z. 2002. Ab initio protein structure prediction. *Curr. Opin. Struct. Biol.* 12:176–81

43. Henry ER, Eaton WA. 2004. Combinatorial modeling of protein folding kinetics: free energy profiles and rates. *Chem. Phys.* 307:163–85

44. Hiltpold A, Ferrara P, Gsponer J, Caflisch A. 2000. Free energy surface of the helical peptide Y(MEARA)$_6$. *J. Phys. Chem. B* 104:10080–86

45. Horn HW, Swope WC, Pitera JW, Madura JD, Dick TJ, et al. 2004. Development of an improved four-site water model for biomolecular simulations: TIP4P-Ew. *J. Chem. Phys.* 120:9665–78

46. Hubner IA, Oliveberg M, Shakhnovich EI. 2004. Simulation, experiment, and evolution: understanding nucleation in protein S6 folding. *Proc. Natl. Acad. Sci. USA* 101:8354–59

47. Hubner IA, Shimada J, Shakhnovich EI. 2004. Commitment and nucleation in the protein G transition state. *J. Mol. Biol.* 336:745–61

48. Hummer G, García AE, Garde S. 2000. Conformational diffusion and helix formation kinetics. *Phys. Rev. Lett.* 85:2637–40

49. Hummer G, García AE, Garde S. 2001. Helix nucleation kinetics from molecular simulations in explicit solvent. *Proteins* 42:77–84

50. Ivankov DN, Finkelstein AV. 2004. Prediction of protein folding rates from the amino acid sequence-predicted secondary structure. *Proc. Natl. Acad. Sci. USA* 101:8942–44

51. Jang S, Shin S, Pak Y. 2002. Molecular dynamics study of peptides in implicit water: ab initio folding of beta-hairpin, beta-sheet, and beta beta alpha-motif. *J. Am. Chem. Soc.* 124:4976–77

52. Jang S, Shin S, Pak Y. 2003. Replica-exchange method using the generalized effective potential. *Phys. Rev. Lett.* 91:058305

53. Deleted in proof

54. Jorgensen WL, Chandrasekhar J, Madura JD, Impey RW, Klein ML. 1983. Comparison of simple potential functions for simulating liquid water. *J. Chem. Phys.* 79:926–35

55. Jorgensen WL, Maxwell DS, Tirado-Rives J. 1996. Development and testing of the OPLS all-atom force field on conformational energetics and properties of organic liquids. *J. Am. Chem. Soc.* 118:11225–36

56. Jorgensen WL, Tirado-Rives J. 1988. The OPLS potential functions for proteins. Energy minimizations for crystals of cyclic peptides and crambin. *J. Am. Chem. Soc.* 110:1657–66

57. Deleted in proof

58. Klimov DK, Newfield D, Thirumalai D. 2002. Simulations of β-hairpin folding confined to spherical pores using distributed computing. *Proc. Natl. Acad. Sci. USA* 99:8019–24

59. Koga N, Takada S. 2001. Roles of native topology and chain-length scaling in protein folding: a simulation study with a Gō-like model. *J. Mol. Biol.* 313:171–80

60. Krantz BA, Dothager RS, Sosnick TR. 2004. Discerning the structure and energy of multiple transition states in protein folding using Psi-analysis. *J. Mol. Biol.* 337:463–75

61. Krieger F, Fierz B, Bieri O, Drewello M, Kiefhaber T. 2003. Dynamics of unfolded polypeptide chains as model for the earliest steps in protein folding. *J. Mol. Biol.* 332:265–74

61a. Kubelka J, Eaton WA, Hofrichter J. 2003. Experimental tests of villin subdomain folding simulations. *J. Mol. Biol.* 329:625–30

62. Ladurner AG, Itzhaki LS, Daggett V, Fersht AR. 1998. Synergy between simulation and experiment in describing the energy landscape of protein folding. *Proc. Natl. Acad. Sci. USA* 95:8473–78

63. Lapidus LJ, Eaton WA, Hofrichter J. 2000. Measuring the rate of intramolecular contact formation in polypeptides. *Proc. Natl. Acad. Sci. USA* 97:7220–25

64. Lee SY, Fujitsuka Y, Kim do H, Takada S. 2004. Roles of physical interactions in determining protein-folding mechanisms: molecular simulation of protein G and alpha spectrin SH3. *Proteins* 55:128–38

65. Levitt M. 1990. *ENCAD, Energy Calculations and Dynamics*. Palo Alto, CA: Molecular Applications Group

66. Levitt M, Hirshberg M, Sharon R, Laidig KE, Daggett V. 1997. Calibration and testing of a water model for simulation of the molecular dynamics of proteins and nucleic acids in solution. *J. Phys. Chem. B* 101:5051–61

67. Li A, Daggett V. 1994. Characterization of the transition state of protein unfolding by use of molecular dynamics: chymotrypsin inhibitor 2. *Proc. Natl. Acad. Sci. USA* 91:10430–34

68. Li A, Daggett V. 1996. Identification and characterization of the unfolding transition state of chymotrypsin inhibitor 2 by molecular dynamics simulations. *J. Mol. Biol.* 257:412–29

69. Li A, Daggett V. 1998. Molecular dynamics simulation of the unfolding of barnase: characterization of the major intermediate. *J. Mol. Biol.* 275:677–94

70. Li L, Shakhnovich EI. 2001. Constructing, verifying, and dissecting the folding transition state of chymotrypsin inhibitor 2 with all-atom simulations. *Proc. Natl. Acad. Sci. USA* 98:13014–18

71. Li PC, Makarov DE. 2004. Ubiquitin-like protein domains show high resistance to mechanical unfolding similar to that of the 127 domain in titin: evidence from simulations. *J. Phys. Chem. B* 108:745–49

72. MacKerell AD Jr, Bashford D, Bellott M, Dunbrack RL Jr, Evanseck JD, et al. 1998. All-atom empirical potential for molecular modeling and dynamics studies of proteins. *J. Phys. Chem. B* 102:3586–616

73. Makarov DE, Keller CA, Plaxco KW, Metiu H. 2002. How the folding rate constant of simple, single-domain proteins depends on the number of native contacts. *Proc. Natl. Acad. Sci. USA* 99:3535–39

74. Makarov DE, Metiu H. 2002. A model for the kinetics of protein folding: kinetic Monte Carlo simulations and analytical results. *J. Chem. Phys.* 116:5205–16

75. Mayor U, Guydosh NR, Johnson CM, Grossmann JG, Sato S, et al. 2003. The complete folding pathway of a protein from nanoseconds to microseconds. *Nature* 421:863–67

76. Mayor U, Johnson CM, Daggett V, Fersht AR. 2000. Protein folding and unfolding in microseconds to nanoseconds by experiment and simulation. *Proc. Natl. Acad. Sci. USA* 97:13518–22

77. Mitsutake A, Sugita Y, Okamoto Y. 2001. Generalized-ensemble algorithms for molecular simulations of biopolymers. *Biopolymers* 60:96–123

78. Muñoz V, Eaton WA. 1999. A simple model for calculating the kinetics of protein folding from three-dimensional structures. *Proc. Natl. Acad. Sci. USA* 96:11311–16

79. Muñoz V, Thompson PA, Hofrichter J, Eaton WA. 1997. Folding dynamics and mechanism of beta-hairpin formation. *Nature* 390:196–99

80. Paci E, Cavalli A, Vendruscolo M, Caflisch A. 2003. Analysis of the distributed computing approach applied to the folding of a small beta peptide. *Proc. Natl. Acad. Sci. USA* 100:8217–22

81. Pan Y, Daggett V. 2001. Direct comparison of experimental and calculated folding free energies for hydrophobic deletion

mutants of chymotrypsin inhibitor 2: free energy perturbation calculations using transition and denatured states from molecular dynamics simulations of unfolding. *Biochemistry* 40:2723–31

82. Pande VS, Baker I, Chapman J, Elmer S, Kaliq S, et al. 2003. Atomistic protein folding simulations on the submillisecond timescale using worldwide distributed computing. *Biopolymers* 68:91–109

83. Pitera JW, Swope W. 2003. Understanding folding and design: replica-exchange simulations of "Trp-cage" fly miniproteins. *Proc. Natl. Acad. Sci. USA* 100:7587–92

84. Plaxco KW, Baker D. 1998. Limited internal friction in the rate-limiting step of a two-state protein folding reaction. *Proc. Natl. Acad. Sci. USA* 95:13591–96

85. Plaxco KW, Simons KT, Baker D. 1998. Contact order, transition state placement and the refolding rates of single domain proteins. *J. Mol. Biol.* 277:985–94

86. Plaxco KW, Simons KT, Ruczinski I, David B. 2000. Topology, stability, sequence, and length: defining the determinants of two-state protein folding kinetics. *Biochemistry* 39:11177–83

87. Qiu D, Shenkin PS, Hollinger FP, Still WC. 1997. The GB/SA continuum model for solvation. A fast analytical method for the calculation of approximate Born radii. *J. Phys. Chem. A* 101:3005–14

88. Rhee YM, Pande VS. 2003. Multiplexed-replica exchange molecular dynamics method for protein folding simulation. *Biophys. J.* 84:775–86

89. Rhee YM, Sorin EJ, Jayachandran G, Lindahl E, Pande VS. 2004. Simulations of the role of water in the protein-folding mechanism. *Proc. Natl. Acad. Sci. USA* 101:6456–61

90. Sanbonmatsu KY, García AE. 2002. Structure of Met-enkephalin in explicit aqueous solution using replica exchange molecular dynamics. *Proteins* 46:225–34

91. Sanchez IE, Kiefhaber T. 2003. Origin of unusual phi-values in protein folding: evidence against specific nucleation sites. *J. Mol. Biol.* 334:1077–85

92. Sato S, Religa TL, Daggett V, Fersht AR. 2004. Testing protein-folding simulations by experiment: B domain of protein A. *Proc. Natl. Acad. Sci. USA* 101:6952–56

93. Serrano L, Matouschek A, Fersht AR. 1992. The folding of an enzyme. III. Structure of the transition state for unfolding of barnase analyzed by a protein engineering procedure. *J. Mol. Biol.* 224:805–18

94. Shea JE, Brooks CL III. 2001. From folding theories to folding proteins: a review and assessment of simulation studies of protein folding and unfolding. *Annu. Rev. Phys. Chem.* 52:499–535

95. Shea JE, Onuchic JN, Brooks CL III. 1999. Exploring the origins of topological frustration: design of a minimally frustrated model of fragment B of protein A. *Proc. Natl. Acad. Sci. USA* 96:12512–17

96. Shea JE, Onuchic JN, Brooks CL III. 2002. Probing the folding free energy landscape of the Src-SH3 protein domain. *Proc. Natl. Acad. Sci. USA* 99:16064–68

97. Sheinerman FB, Brooks CL III. 1998. Calculations on folding of segment B1 of streptococcal protein G. *J. Mol. Biol.* 278:439–56

98. Sheinerman FB, Brooks CL III. 1998. Molecular picture of folding of a small alpha/beta protein. *Proc. Natl. Acad. Sci. USA* 95:1562–67

99. Shimada J, Shakhnovich EI. 2002. The ensemble folding kinetics of protein G from an all-atom Monte Carlo simulation. *Proc. Natl. Acad. Sci. USA* 99:11175–80

100. Shirts MR, Pande VS. 2001. Mathematical analysis of coupled parallel simulations. *Phys. Rev. Lett.* 86:4983–87

101. Simmerling C, Strockbine B, Roitberg AE. 2002. All-atom structure prediction and folding simulations of a stable protein. *J. Am. Chem. Soc.* 124:11258–59

102. Singhal N, Snow CD, Pande VS. 2004. Using path sampling to build better Markovian state models: predicting the

folding rate and mechanism of a trypto-phan zipper beta hairpin. *J. Chem. Phys.* 121:415–25

103. Snow CD, Nguyen H, Pande VS, Gruebele M. 2002. Absolute comparison of simulated and experimental protein-folding dynamics. *Nature* 420:102–6

104. Snow CD, Qiu L, Du D, Gai F, Hagen SJ, Pande VS. 2004. Trp zipper folding kinetics by molecular dynamics and temperature-jump spectroscopy. *Proc. Natl. Acad. Sci. USA* 101:4077–82

105. Sorin EJ, Pande VS. 2005. Exploring the helix-coil transition via all-atom equilibrium ensemble simulations. *Biophys. J.* In press

106. Sorin EJ, Rhee YM, Nakatani BJ, Pande VS. 2003. Insights into nucleic acid conformational dynamics from massively parallel stochastic simulations. *Biophys. J.* 85:790–803

107. Sugita Y, Kitao A, Okamoto Y. 2000. Multidimensional replica-exchange method for free-energy calculations. *J. Chem. Phys.* 113:6042–51

108. Sugita Y, Okamoto Y. 1999. Replica-exchange molecular dynamics method for protein folding. *Chem. Phys. Lett.* 314:141–51

109. Swope WC, Pitera JW, Suits FJ. 2004. Describing protein folding kinetics by molecular dynamics simulations. 1. Theory. *J. Phys. Chem. B* 108:6571–81

110. Swope WC, Pitera JW, Suits FJ, Pitman M, Eleftheriou M, et al. 2004. Describing protein folding kinetics by molecular dynamics simulations. 2. Example applications to alanine dipeptide and a beta-hairpin peptide. *J. Phys. Chem. B* 108:6582–94

111. Thompson PA, Munoz V, Jas GS, Henry ER, Eaton WA, Hofrichter J. 2000. The helix-coil kinetics of a heteropeptide. *J. Phys. Chem. B* 104:378–89

112. Williams S, Causgrove TP, Gilmanshin R, Fang KS, Callender RH, et al. 1996. Fast events in protein folding: helix melting and formation in a small peptide. *Biochemistry* 35:691–97

113. Wolynes PG. 2004. Latest folding game results: Protein A barely frustrates computationalists. *Proc. Natl. Acad. Sci. USA* 101:6837–38

114. Yeh I-C, Hummer G. 2002. Peptide loop-closure kinetics from microsecond molecular dynamics simulations in explicit solvent. *J. Am. Chem. Soc.* 124:6563–68

115. Yun-yu S, Wang L, Gunsteren WFV. 1988. On the approximation of solvent effects on the conformation and dynamics of cyclosporin A by stochastic dynamics simulation techniques. *Mol. Simul.* 1:369–83

116. Zagrovic B, Pande V. 2003. Solvent viscosity dependence of the folding rate of a small protein: distributed computing study. *J. Comp. Chem.* 24:1432–36

117. Zagrovic B, Snow CD, Shirts MR, Pande VS. 2002. Simulation of folding of a small alpha-helical protein in atomistic detail using worldwide-distributed computing. *J. Mol. Biol.* 323:927–37

118. Zagrovic B, Sorin EJ, Pande V. 2001. β-hairpin folding simulations in atomistic detail using an implicit solvent model. *J. Mol. Biol.* 313:151–69

119. Zhou RH. 2003. Free energy landscape of protein folding in water: explicit versus implicit solvent. *Proteins* 53:148–61

120. Zhou RH, Berne BJ. 2002. Can a continuum solvent model reproduce the free energy landscape of a beta-hairpin folding in water? *Proc. Natl. Acad. Sci. USA* 99:12777–82

121. Zhou RH, Berne BJ, Germain R. 2001. The free energy landscape for beta hairpin folding in explicit water. *Proc. Natl. Acad. Sci. USA* 98:14931–36

Contents

ERRATA
　An online log of corrections to *Annual Review of Biophysics and Biomolecular Structure* chapters may be found at http://biophys.annualreviews.org/errata.shtml